IL NUOVO CIMENTO **42 C** (2019) 89
DOI 10.1393/ncc/i2019-19089-6

Colloquia: EuNPC 2018

Nuclear structure solving problems of fundamental physics

J. Suhonen(*)
University of Jyvaskyla, Department of Physics - P.O. Box 35, 40014, Finland

received 5 February 2019

Summary. — Nuclear-structure calculations are important inputs for solving problems of fundamental physics. Such problems are related with, e.g., neutrinos and dark-matter particles and their interactions with atomic nuclei. In this article the focus is directed to the important problem of the renormalization of the weak axial coupling $g_{\rm A}$ and accurate treatment of β spectrum shapes. As particular applications of the spectral shapes the spectrum-shape method (SSM) and the hot topic of "reactor antineutrino anomaly" are introduced.

1. – Introduction

The parity non-conserving nature of the weak interaction forces the hadronic current $J^\mu_{\rm H}$ to be written at the quark level as a mixture of vector and axial-vector parts:

$$J^\mu_{\rm H} = \bar{q}_f(x)\gamma^\mu(1-\gamma_5)q_i(x)\,, \tag{1}$$

where q_i (q_f) is the initial-state (final-state) quark. Renormalization effects of strong interactions and energy scale of the processes must be taken into account when moving from the quark level to the hadron level. Then the hadronic current between nucleons N_i and N_f can be written for low-energy (in the scale of few MeV) nuclear processes as

$$J^\mu_{\rm H} = \bar{N}_f(x)[g_{\rm V}\gamma^\mu - g_{\rm A}\gamma^\mu\gamma_5]N_i(x)\,. \tag{2}$$

Here $g_{\rm V}$ is the vector coupling and $g_{\rm A}$ the axial-vector coupling. For the neutron decay their values are $g_{\rm V} = 1.0$ and $g_{\rm A} = 1.2723(23)$ [1]. In nuclear environment the value $g_{\rm V} = 1.0$ is protected by the conserved vector-current (CVC) hypothesis but $g_{\rm A}$ can be renormalized by *nuclear medium effects* and/or the *nuclear many-body effects*. The former contain quenching related to the presence of spin-multipole giant resonances, non-nucleonic degrees of freedom (like the Δ isobar) and meson-exchange-related two-body weak currents. The latter relates to deficiencies of the nuclear many-body approaches used to compute the wave functions involved in the decay transitions.

(*) E-mail: jouni.suhonen@phys.jyu.fi

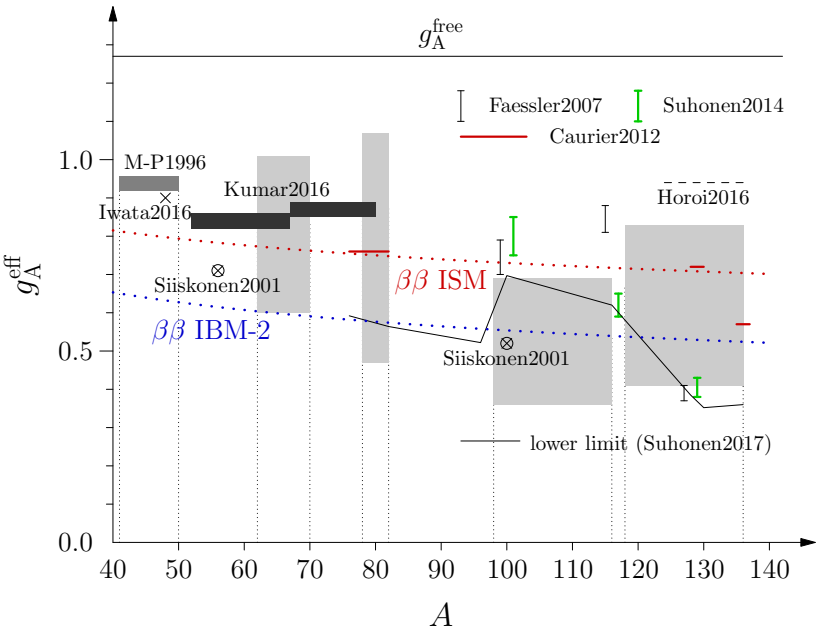

Fig. 1. – Effective values of g_A in different theoretical β and $2\nu\beta\beta$ analyses for the nuclear mass range $A = 41 - 136$. The quoted references are Suhonen2017 [17], Caurier2012 [2], Faessler2007 [13], Suhonen2014 [15] and Horoi2016 [3]. These studies are contrasted with the ISM β-decay studies of M-P1996 [4], Iwata2016 [5], Kumar2016 [6] and Siiskonen2001 [7].

2. – Renormalization of g_A in β and $2\nu\beta\beta$ decays

The renormalization of g_A has long been studied for the Gamow-Teller β decays in the framework of the interacting shell model (ISM). In light of a number of calculations, like the ones of Caurier *et al.* [2], Horoi *et al.* [3], Martínez-Pinedo *et al.* [4], Iwata *et al.* [5], Kumar *et al.* [6] and Siiskonen *et al.* [7], it appears that the value of g_A is quenched, and the stronger the heavier the nucleus. This trend has been depicted in Fig 1 and contrasted against the background of results obtained by the use of the proton-neutron quasiparticle random-phase approximation (pnQRPA) in the works [8-10] (see also [11] and the review [12]). The pnQRPA results constitute the light-hatched regions in the background of the ISM results. The width of the regions reflects the rather large variation of the determined g_A^{eff} for β-decay transitions in different isobaric chains. For more information on the analyses see the review [12]. As can be seen in the figure, the ISM results and the pnQRPA results are commensurate with each other, which is non-trivial considering the large differences in their many-body philosophy.

A simultaneous analysis of the β and two-neutrino double beta ($2\nu\beta\beta$) decays by Faessler *et al.* [13] gave indications of a strongly quenched effective g_A, in the range $g_A^{eff} = 0.39 - 0.84$. These results, along with their 1σ errors, are shown in Fig. 1 as black vertical bars. Later a similar study was carried out in [14, 15], with results comparable with those of [13] and depicted in Fig. 1 as green vertical bars. For more information see the review [12].

Recently the possibly decisive role of g_A in the half-life and discovery potential of the $0\nu\beta\beta$ experiments has surfaced [16, 17]. In Barea *et al.* [16] a comparison of the

experimental and computed $2\nu\beta\beta$ half-lives of a number of nuclei yielded the rather striking result

$$g_{\rm A}^{\rm eff}({\rm IBM\text{-}2}) = 1.269A^{-0.18}\ ; \quad g_{\rm A}^{\rm eff}({\rm ISM}) = 1.269A^{-0.12}\,, \tag{3}$$

where A is the mass number and IBM-2 stands for the microscopic interacting boson model. The IBM-2 results have been obtained by using the closure approximation for the analyzed $2\nu\beta\beta$ transitions since there are no spin-isospin degrees of freedom in the theory framework. The results (3), depicted in Fig. 1 as red (ISM) and blue (IBM-2) dotted curves, are in nice agreement with the trends shown by the ISM and pnQRPA analyses mentioned before.

One can conclude that all the mentioned analyses strongly point to a quenched value of $g_{\rm A}$ and the quenching is mass-number dependent, increasing with increasing A.

3. – Spectral shapes of forbidden β decays

The half-life of forbidden non-unique β decays can be written in the form

$$t_{1/2} = \kappa/\tilde{C}\,, \tag{4}$$

where $\tilde{C}$ is the dimensionless integrated shape function, given by

$$\tilde{C} = \int_1^{w_0} C(w_e) p_e w_e (w_0 - w_e)^2 F_0(Z_f, w_e) {\rm d}w_e\,. \tag{5}$$

Here w_e is the total energy of the emitted electron/positron, w_0 is the endpoint energy, p_e is the electron/positron momentum, Z_f is the atomic number of the daughter nucleus and $F_0(Z_f, w_e)$ is the Fermi function taking into account the coulombic attraction/repulsion of the electron/positron and the daughter nucleus. The shape factor $C(w_e)$ in (5) can be decomposed into vector, axial-vector and mixed vector-axial-vector parts in the form [18]

$$C(w_e) = g_{\rm V}^2 C_{\rm V}(w_e) + g_{\rm A}^2 C_{\rm A}(w_e) + g_{\rm V} g_{\rm A} C_{\rm VA}(w_e)\,. \tag{6}$$

In [18] it was found that the shapes of β spectra could be used to determine the effective values of the weak coupling strengths $g_{\rm V}$ and $g_{\rm A}$ by comparing the computed spectrum with the measured one for forbidden non-unique β decays. This method was coined the spectrum-shape method (SSM)([1]). The work of [18] was extended to other nuclei and nuclear models in [19-21]. In all these studies it was found that the SSM is quite robust, not very sensitive to the adopted mean field or nuclear many-body model and its model Hamiltonian.

Examples of possible $g_{\rm A}$ dependencies are given in the three-panel Fig. 2, where the ISM-computed first-forbidden non-unique ground-state-to-ground-state β^- decays of ^{207}Tl [panel (a)], ^{210}Bi [panel (b)] and ^{214}Bi [panel (c)] are depicted. The β-spectrum shapes of ^{207}Tl and ^{214}Bi are only slightly $g_{\rm A}$ dependent, but for ^{210}Bi the dependence is extremely strong. This makes ^{210}Bi an excellent candidate for the application of the SSM

([1]) In fact, the spectrum shape depends on the ratio $g_{\rm V}/g_{\rm A}$ but the decay rate, and thus the half-life, depends on the absolute values of these weak couplings.

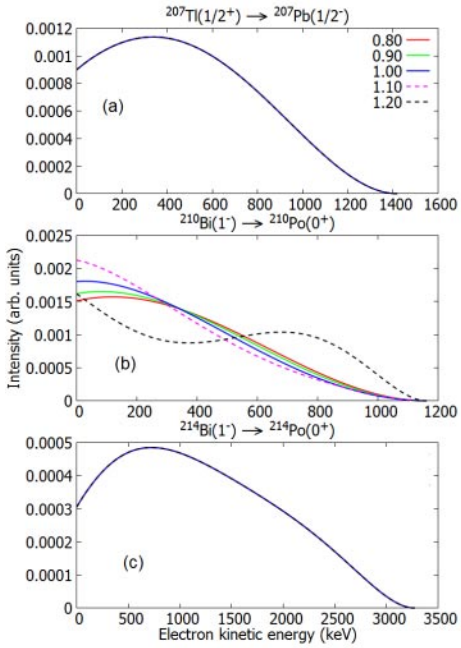

Fig. 2. – Normalized β spectra for the first-forbidden non-unique ground-state-to-ground-state β^- decays of ^{207}Tl [panel (a)], ^{210}Bi [panel (b)] and ^{214}Bi [panel (c)]. The value $g_{\rm V} = 1.00$ was adopted in the calculations and the color coding represents the different adopted values for $g_{\rm A}$ (for the cases of panels (a) and (c) all the colored lines overlap in the adopted scales of the figures). Note also the Coulomb shift of the spectra.

once new measurement(s) of the spectrum shape are performed. This is so far the only known first-forbidden β transition with a strong $g_{\rm A}$ dependence. Other thus far found strongly $g_{\rm A}$-dependent decay transitions are listed in Table I. There the branchings to the indicated final states are practically 100% in all cases and the sensitivity to the value of $g_{\rm A}$ is at the same level as shown in Fig. 2, panel (b), except for the decay of ^{87}Rb which is only moderately sensitive to $g_{\rm A}$.

4. – β-spectrum shapes and the reactor-antineutrino anomaly

One direct application of the β-spectrum shapes is the reactor antineutrino anomaly (RAA) [23]. In the RAA the measured antineutrino fluxes emanating from the fission products of nuclear reactors are lower than the fluxes deduced from nuclear data [24]. In addition, there is a strange "bump" between 4 and 6 MeV in the measured antineutrino spectrum. The RAA and the spectral bump have been measured in the neutrino-oscillation experiments Daya Bay [25], RENO [26] and Double Chooz [27]. The measured flux is some 6(2)% lower than predicted by nuclear data thus making this a rough 3σ effect [25]. The method of virtual β branches [28] has been used to estimate the cumulative β spectra responsible for the theoretical antineutrino flux. The involved β decays go partly by forbidden transitions that cannot be assessed by the present nuclear data, but instead, could be calculated.

TABLE I. – *Selected forbidden non-unique β^--decay transitions and their sensitivity to the value of g_A. Here J_i (J_f) is the angular momentum of the initial (final) state, π_i (π_f) the parity of the initial (final) state, and K the degree of forbiddenness (column 4). The initial state is always the ground state (gs, column 2) and the final state is either the ground state (gs) or the $n_f : th$, $n_f = 1, 2, 3$, excited state (column 3) of the daughter nucleus. The last column lists the nuclear models which have been used (thus far) to compute the β-spectrum shape. Here also references to the original works are given.*

Transition	$J_i^{\pi_i}$ (gs)	$J_f^{\pi_f}$ (n_f)	K	Nucl. model
^{87}Rb $\rightarrow$ ^{87}Sr	$3/2^-$	$9/2^+$ (gs)	3	MQPM [20], ISM [21]
^{94}Nb $\rightarrow$ ^{94}Mo	6^+	4^+ (2)	2	ISM [21]
^{98}Tc $\rightarrow$ ^{98}Ru	6^+	4^+ (3)	2	ISM [21]
^{99}Tc $\rightarrow$ ^{99}Ru	$9/2^+$	$5/2^+$ (gs)	2	MQPM [20], ISM [21]
^{113}Cd $\rightarrow$ ^{113}In	$1/2^+$	$9/2^+$ (gs)	4	MQPM [18, 20], ISM [18], IBFM-2 [19]
^{115}In $\rightarrow$ ^{115}Sn	$9/2^+$	$1/2^+$ (gs)	4	MQPM [18, 20], ISM [19], IBFM-2 [19]
^{138}Cs $\rightarrow$ ^{138}Ba	3^-	3^+ (1)	1	ISM [22]
^{210}Bi $\rightarrow$ ^{210}Po	1^-	0^+ (gs)	1	ISM (this work)

The cumulative β spectra consist of numerous decay branches but not all of them contribute equally, thus allowing a fit by just a limited number of virtual β spectra emerging from non-existent fictional β branches [28, 29]. A shortcoming of this procedure is that all the virtual branches are assumed to be described by allowed β-spectrum shapes. Also adding information from the nuclear databases is not accurate enough due to deficiencies in this information. Out of the several thousand β branches taking part in the cumulative β spectra the majority are allowed decays but the contribution from the first-forbidden decay transitions is also considerable, in particular in the interesting region of the antineutrino spectrum, between 4 and 6 MeV [30]. On the other hand,

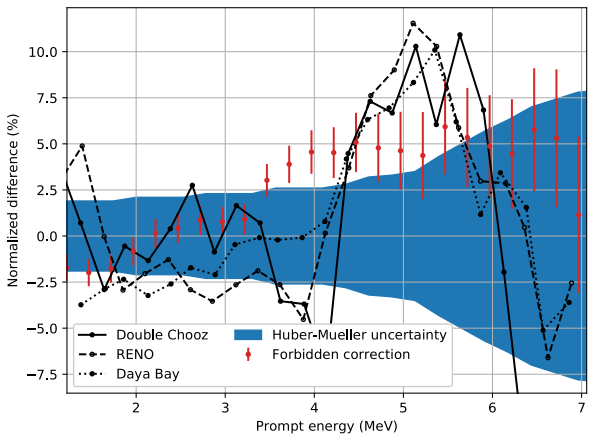

Fig. 3. – Normalized spectral ratios for the three neutrino-oscillation experiments relative to the Mueller [24] predictions. The red vertical bars give the normalized spectrum by including the information obtained from the calculated spectral shapes of first-forbidden β transitions.

forbidden decays become increasingly unlikely with increasing degree of forbiddenness.

The RAA has been associated to disappearance of electron antineutrinos in short-baseline (10−100 m) reactor oscillation experiments. The disappearance can be explained quantitatively, e.g., by existence of sterile neutrinos. A $3+1$ scheme, with one sterile neutrino in eV mass scale, could explain the anomaly [31]. In [30] it was found that both the effect of the RAA and the spectral "bump" is drastically mitigated by the ISM-calculated spectrum shapes for 29 key first-forbidden transitions and a subsequent Monte Carlo analysis for the rest of the first-forbidden transitions. This offers a possible nuclear-physics explanation of the RAA and the "bump". This mitigation is demonstrated in Fig. 3 where the measured flux by the three mentioned experiments is compared with the Mueller [24] prediction and the result of the analysis performed in [30].

* * *

This work has been partially supported by the Academy of Finland under the Academy project no. 318043.

REFERENCES

[1] Patrignani C. *et al.* (Particle Data Group), *Chin. Phys. C*, **40** (2016) 100001.
[2] Caurier E. *et al.*, *Phys. Lett. B*, **711** (2012) 62.
[3] Horoi M. and Neacsu A., *Phys. Rev. C*, **93** (2016) 024308.
[4] Martínez-Pinedo G. *et al.*, *Phys. Rev. C*, **53** (1996) R2602.
[5] Iwata Y. *et al.*, *Phys. Rev. Lett.*, **116** (2016) 112502.
[6] Kumar V. *et al.*, *J. Phys. G: Nucl. Part. Phys.*, **43** (2016) 105104.
[7] Siiskonen T. *et al.*, *Phys. Rev. C*, **63** (2001) 055501.
[8] Ejiri H. and Suhonen J., *J. Phys. G: Nucl. Part. Phys.*, **42** (2015) 055201.
[9] Pirinen P. and Suhonen J., *Phys. Rev. C*, **91** (2015) 054309.
[10] Deppisch F. F. and Suhonen J., *Phys. Rev. C*, **94** (2016) 055501.
[11] Delion D. S. and Suhonen J., *Europhys. Lett.*, **107** (2014) 52001.
[12] Suhonen J., *Front. in Phys.*, **5** (2017) 55.
[13] Faessler A. *et al.*, *J. Phys. G: Nucl. Part. Phys.*, **35** (2008) 075104.
[14] Suhonen J. and Civitarese O., *Phys. Lett. B*, **725** (2013) 153.
[15] Suhonen J. and Civitarese O., *Nucl. Phys. A*, **924** (2014) 1.
[16] Barea J. *et al.*, *Phys. Rev. C*, **87** (2013) 014315.
[17] Suhonen J., *Phys. Rev. C*, **96** (2017) 055501.
[18] Haaranen M. *et al.*, *Phys. Rev. C*, **93** (2016) 034308.
[19] Haaranen M. *et al.*, *Phys. Rev. C*, **95** (2017) 024327.
[20] Kostensalo J. *et al.*, *Phys. Rev. C*, **95** (2017) 044313.
[21] Kostensalo J. and Suhonen J., *Phys. Rev. C*, **96** (2017) 024317.
[22] Kostensalo J. and Suhonen J., *Phys. Lett. B*, **781** (2018) 480.
[23] Buck C. *et al.*, *Phys. Lett. B*, **765** (2017) 159.
[24] Mueller T. A. *et al.*, *Phys. Rev. C*, **83** (2011) 054615.
[25] An F. P. *et al.* (Daya Bay Collaboration), *Phys. Rev. Lett.*, **118** (2017) 251801.
[26] Ahn J. K. *et al.* (RENO Collaboration), *Phys. Rev. Lett.*, **108** (2012) 191802.
[27] Abe Y. *et al.* (Double Chooz Collaboration), *J. High Energy Phys.*, **2014(10)** (2014) 86.
[28] Schreckenbach K. *et al.*, *Phys. Lett. B*, **160** (1985) 325.
[29] Sonzogni A. A. *et al.*, *Phys. Rev. Lett.*, **119** (2017) 112501.
[30] Hayen L. *et al.*, *arXiv*, **1805.12259** (2018) [nucl-th].
[31] Giunti C. *et al.*, *Phys. Rev. D*, **86** (2012) 113014.